

RESEARCH

Open Access



A strain of *Lactobacillus plantarum* from piglet intestines enhances the anti-PoRV effect via the STING-IFN-I pathway

Anqi Sun^{1†}, Xin Shan^{1†}, Ruihan Liu¹, Zhengxu Tang¹, Jingshu Huang¹, Shihan Zhang¹, Lihong Bian¹, Yumeng Shi¹, Zixuan Liu¹, Jingtao Hu^{1*} and Chunfeng Wang^{1*}

Abstract

Background Rotavirus infection represents a major etiology of severe diarrheal disease in neonatal and weaned piglets, causing substantial economic burdens to the global swine industry. *Lactobacillus plantarum*, a ubiquitous probiotic in natural ecosystems, has demonstrated multifaceted biological functions. The stimulator of the interferon gene (STING) is involved in type I interferon (IFN-I) mediated host antiviral innate immunity, which is a pivotal adaptor in response to the microbial DNA/RNA-activated signaling pathways. Emerging evidence suggests that certain probiotic strains can activate the STING-dependent pathway to induce IFN-I responses. In the present study, we successfully isolated a strain of *Lactobacillus plantarum* (designated LP1) from porcine intestinal contents and investigate its potential to counteract porcine rotavirus (PoRV) infection via modulation of antiviral signaling pathway.

Result LP1 exhibited superior tolerance to simulated gastrointestinal conditions (pH 3.0 and 0.3% bile salts) compared with other isolated *Lactobacillus* strains. In vitro adhesion assays demonstrated that LP1 effectively colonized porcine intestinal epithelial cells (IPEC-J2) without inducing cytotoxicity or apoptosis. Animal experiments also confirmed the protective effect of LP1 in mice against rotavirus, by reducing body weight loss, promoting viral clearance in feces, and alleviating intestinal mucosal damage. Mechanistic investigations identified STING-IRF3 pathway activation as the pivotal antiviral mechanism. Both phosphorylation of STING and IRF3 in LP1-treated IPEC-J2 cells accompanied by upregulated transcription and secretion of IFN- β and interferon-stimulated genes (ISGs). Consistent findings were observed in intestinal tissues of LP1-protected mice with STING pathway activation correlating with reduction in viral titers. Crucially, STING inhibitor (C-170) administration could reverse LP1-mediated antiviral effects.

Conclusion LP1 exerts potent anti-PoRV activity in both murine models and porcine intestinal epithelial (IPEC-J2) cells through STING-IRF3 signaling axis-mediated IFN- β production.

Keywords Anti-PoRV effect, *Lactobacillus plantarum*, STING-IFN-I pathway

[†]Anqi Sun and Xin Shan contributed equally to this work.

*Correspondence:

Jingtao Hu
jingtaoh@jlau.edu.cn
Chunfeng Wang
wangchunfeng@jlau.edu.cn

¹College of Veterinary Medicine, Jilin Provincial Engineering Research Center of Animal Probiotics, Jilin Provincial Key Laboratory of Animal Microecology and Healthy Breeding, Engineering Research Center of Microecological Vaccines (Drugs) for Major Animal Diseases, Ministry of Education, Jilin Agricultural University, Changchun 130118, China



© The Author(s) 2025. **Open Access** This article is licensed under a Creative Commons Attribution-NonCommercial-NoDerivatives 4.0 International License, which permits any non-commercial use, sharing, distribution and reproduction in any medium or format, as long as you give appropriate credit to the original author(s) and the source, provide a link to the Creative Commons licence, and indicate if you modified the licensed material. You do not have permission under this licence to share adapted material derived from this article or parts of it. The images or other third party material in this article are included in the article's Creative Commons licence, unless indicated otherwise in a credit line to the material. If material is not included in the article's Creative Commons licence and your intended use is not permitted by statutory regulation or exceeds the permitted use, you will need to obtain permission directly from the copyright holder. To view a copy of this licence, visit <http://creativecommons.org/licenses/by-nc-nd/4.0/>.

Background

Rotavirus is a leading cause of life-threatening diarrheal disease in neonatal animals across a broad range of mammalian species, imposing substantial economic and health burdens globally [1]. The virus transmits through multiple routes, including fecal-oral, respiratory, and potentially other less-characterized pathways [2]. It preferentially infects intestinal epithelial cells, leading to the disruption of mucosal barrier integrity and the onset of severe gastroenteritis [3, 4]. Mounting evidence indicates that rotaviruses are capable of crossing species barriers, posing considerable zoonotic threats to both livestock and human [4, 5]. Current vaccination strategies face challenges due to loss of efficacy associated with the genetic diversity of circulating rotavirus strains [6]. In light of these limitations, probiotics have emerged as promising adjuncts in antiviral defense, offering protective effects against enteric infections in animals [7–9]. These commensal microorganisms exert their antiviral functions through dual mechanisms: stimulating innate immune responses and mitigating pathogen-induced intestinal inflammation [10–13].

Among probiotic candidates, *Lactobacillus plantarum* exhibits multifaceted protective effects against intestinal pathogens. Experimental evidence indicates that this strain can suppress the expression of pro-inflammatory mediators such as Toll-like receptor 4 (TLR4), IL-6, and TNF α , while enhancing the integrity of the jejunal mucosal barrier during enteric infections [14]. Its anti-inflammatory potential is further supported by the inhibition of key signaling cascades, including the NF- κ B and MAPK pathways [15]. Notably, this strain demonstrates broad-spectrum antiviral activity, with documented inhibition of transmissible gastroenteritis coronavirus replication through metabolite-mediated mechanisms [16]. Both viable cells and cell-free culture supernatants of *Lactobacillus plantarum* show efficacy against porcine epidemic diarrhea virus in experimental models [17]. Moreover, extracellular polysaccharides derived from this species

significantly reduce rotavirus infection rates in animal challenge models [18]. Despite these promising findings, the precise molecular mechanisms by which *Lactobacillus plantarum* confers antiviral protection remain incompletely understood.

STING (stimulator of interferon genes) functions as a central adaptor protein in innate antiviral immunity. Upon activation, STING recruits and activates TANK-binding kinase 1 (TBK1), which in turn phosphorylates interferon regulatory factor 3 (IRF3), leading to transcriptional induction of type I interferons (IFN-I). Although initially characterized as a downstream effector of cGAS-mediated cytosolic DNA sensing, STING is now increasingly recognized for its role in RNA virus detection across diverse mammalian systems. For instance, Cheng et al. reported that STING inhibits replication of H9N2 avian influenza virus in duck embryo fibroblasts [19]. Commensal gut microbiota mediates constitutive activation of the cGAS-STING-IFN-I axis, establishing fundamental antiviral immunity against both DNA and RNA viruses. For example, specific probiotic strains *Lactobacillus plantarum* WCFS-1 and *Pediococcus pentosaceus* NCTC 990 elicit STING-mediated type I interferon production through the cGAS-STING signaling axis in human macrophage-like cells and primary phagocytes [20]. Building on these insights, we performed a series of in vitro and in vivo studies to assess the antiviral potential of a porcine-derived *Lactobacillus plantarum* strain (LP1). Our data demonstrate that LP1 confers protection against porcine rotavirus (PoRV) infection by activating the STING–IFN-I signaling axis. These findings offer a mechanistic framework for probiotic-based interventions targeting enteric viral pathogens.

Result

Isolation and characterization of *Lactobacillus*

Fecal samples and intestinal mucosa specimens were collected from healthy piglets inhabiting porcine rotavirus (PoRV)-endemic farms for microbial characterization. Through 16 S rDNA sequencing analysis, we successfully isolated and identified 21 distinct *Lactobacillus* strains, including *Lactobacillus plantarum* (abbreviated LP), *Lactobacillus reuteri* (abbreviated LR), *Lactobacillus amylovorus* (abbreviated LA), *Lactobacillus acidophilus* (abbreviated LAA), and *Lactobacillus mucosa* (abbreviated LM) (Table 1). Subsequently, four strains including LP1, LP013, LR005, and LR50 exhibited remarkable resistance to both low-pH conditions and bile salt exposure. Quantitative analysis demonstrated that LP1 maintained viability at 1.0×10^7 CFU/mL after 2-hour incubation in pH 3.0 medium. Notably, this strain achieved a survival rate of 1.0×10^8 CFU/mL following treatment with 0.3% (w/v) bile salts. In comparison with other isolated

Table 1 Isolation of lactic acid bacteria strains from piglet feces and intestine

Samples	Number of strains	Number of <i>Lactobacillus</i> strain	Types and name of strain
Intestine	182	20	<i>Lactobacillus plantarum</i> : LP1, LP013 <i>Lactobacillus reuteri</i> : LR50, LR68, LR005, LR71, LR114 <i>Lactobacillus amylovorus</i> : LA25 <i>Lactobacillus vaginalis</i> : LV1, LV2... LV11 <i>Lactobacillus acidophilus</i> : LAA012 <i>Lactobacillus mucosa</i> : LM46
Feces	111	1	<i>Lactococcus lactis</i> : LL3

strains, LP1 possessed superior gastrointestinal tolerance (Table 2).

Whole genome sequencing analysis

Here, the genome of *Lactobacillus plantarum* LP1 was sequenced using the Illumina Hiseq Novaseq and PacBio Sequel platform. A total of 1,321,986,300 raw data was generated from two DNA libraries: a pair-end library with an insert size of 500 bp and a mate-pair library with an insert size of 20 kb. The estimated genome size of LP1 strain was calculated to be 3,219,416 bp with a GC content of 44.57% (Table 3; Fig. 1a). In addition, 3034 open reading frames of protein coding genes could be annotated, the number of bases occupied by the open reading frames 26,928,663 bp, the total length of the open reading frames accounted for 83.64% of the genome length, the total length of intergenic regions accounted for 16.36% of the genome length, the average GC content of open reading frames was 45.68%, the average GC content of intergenic regions was 38.89% (Table 4). The protein coding genes were annotated by COG, it was found that a total of 2583 protein coding genes were annotated (Fig. 1b), which could be categorized into 24 classes from A~Z. Among them, the number of genes with unknown function was 640, accounting for 21.0943% of the total number of annotated genes, 260 genes of annotated transcription were accounting for 8.5695% respectively, 61 genes involved in defense mechanisms were annotated, 41 genes were encoding ABC transporters. GO analysis results show that there were 2002, 2074 and 775 functional genes annotated to molecular function, biological process and cellular component, respectively (Fig. 1c). The GO function was annotated on molecular function, ion binding, biological processes, cellular nitrogen compound metabolic processes and biosynthetic processes, cellular function and cellular components. Comparative analysis of chr with KEGG database showed that there were 2261 genes corresponding to KEGG Pathway, which were involved in 45 metabolic pathways (Fig. 1d). The results of KEGG enrichment analysis showed that genetic information processing in protein families (449 genes), signaling and cellular process (369 genes), and carbohydrate metabolism (293 genes) were the three most important metabolic pathways respectively.

Effect of LP1 on cell viability, apoptosis and adhesive capacity

Cellular viability and apoptotic responses were evaluated in IPEC-J2 cells through CCK-8 assays and flow cytometry following LP1 inoculation at ratios of 10:1 and 100:1 (bacteria-to-cell) for 1, 4, or 6 h (Fig. 2). Notably, cells exposed to LP1 for 1 h exhibited mild but non-significant enhancement in viability compared to LP-untreated cells (control) (Fig. 2a). Prolonged exposure (4–6 h) to LP1 (at

Table 2 Determination of acid and bile salt resistance

Strain samples	Vaible count (CFU)	Vaible count after pH= 3.0 treatment for 2 h (CFU)	Vaible count after 0.3% bile salt treatment for 2 h (CFU)
LP1	1×10^9	1×10^7	1.0×10^8
LP013	1×10^9	1.5×10^6	1.0×10^7
LR50	1×10^9	1×10^6	1.0×10^7
LR68	1×10^9	1×10^5	1.0×10^6
LR005	1×10^9	1.1×10^6	1.0×10^7
LR71	1×10^9	1.1×10^5	1.0×10^6
LR114	1×10^9	1.6×10^5	1.0×10^6
LAA012	1×10^9	1.4×10^5	1.0×10^6
LM46	1×10^9	1.2×10^5	1.0×10^6
LA25	1×10^9	1.3×10^5	1.0×10^6
LV1	1×10^9	1.1×10^4	1.0×10^7
LV2	1×10^9	1.1×10^5	1.0×10^6
LV3	1×10^9	1×10^5	1.0×10^6
LV4	1×10^9	1×10^5	1.0×10^6
LV5	1×10^9	1×10^5	0
LV6	1×10^9	0	1.0×10^6
LV7	1×10^9	1×10^5	1.0×10^6
LV8	1×10^9	0	1.0×10^6
LV9	1×10^9	1×10^5	1.0×10^6
LV10	1×10^9	0	0
LV11	1×10^9	1×10^5	1.0×10^6

Table 3 Data statistics of genome assembly

Sample	Seq Length(bp)	GC Content (%)
LP1	3,219,416	44.57

a ratio of 100:1) still maintained cellular viability levels comparable to control (Fig. 2b). Flow cytometric quantification confirmed the absence of LP1-induced apoptosis across all treatment groups when compared to control (Fig. 2c-d). To characterize bacterial adhesion capacity, CFSE-labeled LP1 was visualized via fluorescence microscopy and quantified through colony-forming unit (CFU) enumeration. Significantly enhanced bacterial colonization was observed in cells incubated with LP1 for 6 h compared to the 4 h treatment group, as evidenced by both increased fluorescent signal intensity ($p < 0.01$) and elevated viable bacterial counts ($p < 0.01$) (Fig. 2e-f). These findings collectively demonstrate that LP1 possesses adhesion capacity toward porcine intestinal epithelial cells.

Protective effects of LP1 on PoRV-infected mice

Mice were orally administered either LP1 or PBS for 7 consecutive days prior to PoRV challenge. Fecal samples were collected daily, and body weight was monitored throughout the experimental period. Our findings indicated that LP1-pretreated mice showed significantly accelerated body weight recovery compared to PBS-treated mice (control) (Fig. 3a-b). Additionally, viral clearance was evident in LP1 group, with fecal viral loads showing a significant reduction at day 3 post-infection compared to control ($p < 0.01$) (Fig. 3c-d).

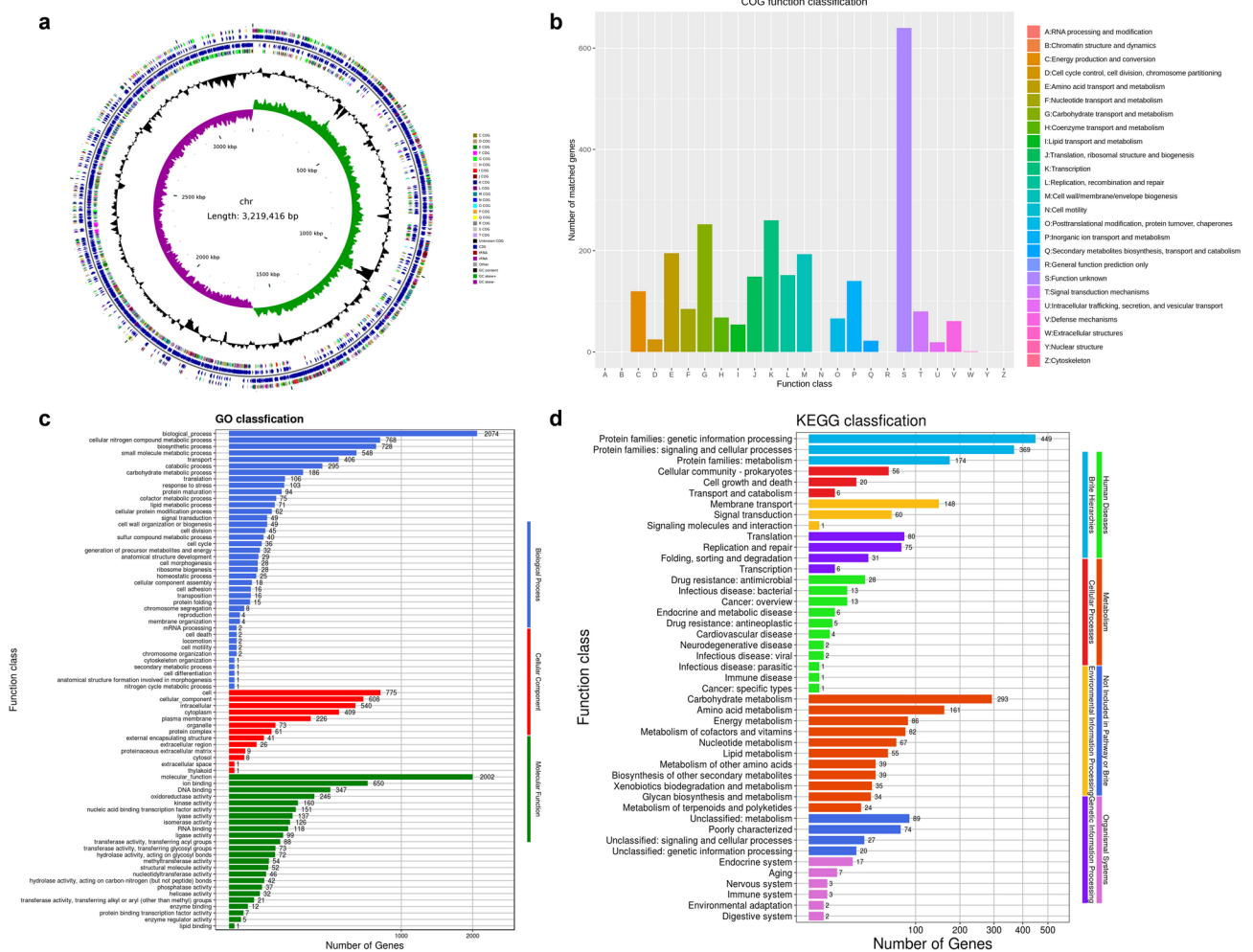


Fig. 1 Whole genome sequencing analysis of LP. (a) Genome circle diagram. (b) COG functional classification. (c) GO annotation map. (d) KEGG statistics

Table 4 Statistics of open reading frame predictions

Sample	Property	Value
LP1	ORF num	3034
	ORF total length	2,692,863 bp
	ORF density	0.942 genes per kb
	Longest ORF length	8142 bp
	ORF average length	887.56 bp
	Intergenic region length	526,553 bp
	ORF/Genome (coding percentage)	83.64%
	Intergenic length/Genome	16.36%
	GC content in ORF region	45.68%
	GC content in intergenic region	38.89

Histopathological assessment further demonstrated the protective effects of LP1 pretreatment, showing marked attenuation of PoRV-induced intestinal damage, including prevention of villus shortening and maintenance of intestinal wall thickness (Fig. 3e).

LP1 activated the STING-IFN-I signaling pathway to trigger IFN-β production

To investigate the immunomodulatory effects of LP1, we assessed IFN-β expression, as well as the phosphorylation of STING and IRF3 in IPEC-J2 cells treated with LP1 (at a ratio of 100) for 4 h and 6 h using qPCR, ELISA and western blotting (Fig. 4). Results demonstrated that IFN-β production was significantly upregulated upon LP1 stimulation ($p < 0.01$) (Fig. 4a-b). Notably, LP1 also enhanced the phosphorylation both STING and IRF3 at 4 h and 6 h, particularly at 6 h ($p < 0.01$) (Fig. 4c-e). These findings collectively revealed that LP1 could enhance activate the STING signaling pathway to trigger IFN-β production, with a more pronounced effect observed at 6 h post-inoculation with IPEC-J2.

LP1 enhanced antiviral effect against PoRV mainly depended on STING

To explore whether the antiviral effect of LP1 primarily relies on STING, IPEC-J2 cells (1×10^6) were pretreated

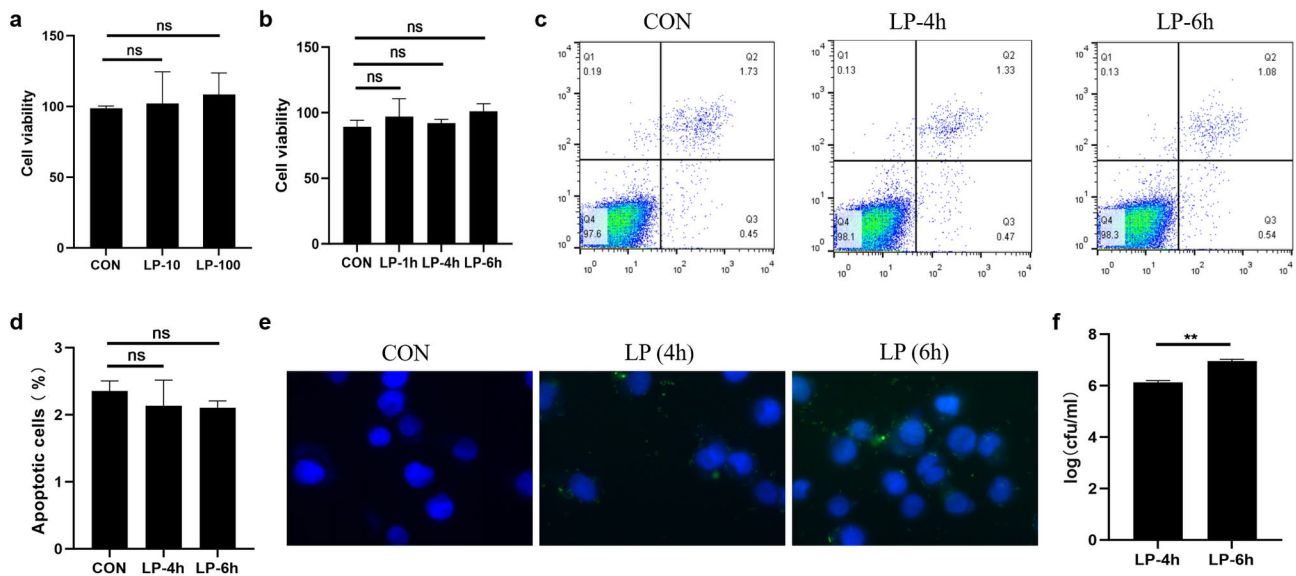


Fig. 2 Effects of LP1 on cell viability, apoptosis and adhesion. **(a)** Cells (1×10^5 cells/well) were initially seeded in 96-well cell culture plates and respectively co-cultured with LP at ratios of 10:1 and 100:1 (bacteria-to-cell) (abbreviated LP-10 and LP-100, respectively) for 1 h by CCK-8 assays. **(b)** Cell viability was respectively determined at a ratio of 100:1 for 1, 4 and 6 h (abbreviated LP-1 h, LP-4 h and LP-6 h). **(c-d)** Effect of LP1 on cell apoptosis by flow cytometry. Cells (2×10^6) were stimulated with LP1 (2×10^8 CFU) for 4 and 6 h, respectively (abbreviated LP-4 h and LP-6 h). **(e-f)** Adherent ability of LP1 on IPEC-J2 cells. **(e)** In order to visually observe the adhesion of LP1 in cells, LP1 labeled with CFSE was observed using a fluorescence microscope. **(f)** The number of bacteria adhering to IPEC-J2 was determined by bacterial plate counting (CFU). All the experiments were repeated three times with similar results. Data are shown as mean \pm SD. * $p < 0.05$, ** $p < 0.01$, ^{ns} no significant

with or without the STING inhibitor C-170 ($1 \mu\text{M}$) for 2 h. Subsequently these cells were incubated with LP1 for 6 h prior to PoRV challenge. The results demonstrated that LP1-pretreatment significantly decreased both viral titer and virus copy number ($p < 0.05$). However, the addition of STING inhibitor resulted in LP1 loss of anti-PoRV activity (Fig. 5a-b). In LP-PoRV group, the phosphorylation of STING (p-STING) and IRF3 (p-IRF3) were both elevated compared to PoRV group ($p < 0.05$). However, these expressions were significantly reduced with the supplementation of C-170 (Fig. 5c-e). Notably, the addition of C-170 also significantly decreased the expression of IFN- β and mRNA transcription, showing as no significant difference between LP-PoRV group and PoRV group (Fig. 5f-g). Furthermore, qPCR indicated that the transcription of IFIT2, CXCL10 and ISG15 was significantly up-regulated in LP-PoRV group. Following interference with C-170, these mRNA were all significantly decreased (Fig. 5h-j). These findings collectively suggested that the STING inhibitor can reverse the antiviral responses of LP1 and revealed that STING played a crucial role in this response.

LP activated STING-IRF3 pathway in mice

Mice was orally infected with PoRV after oral administration of LP1 or PBS for 6 days. Total protein was extracted from jejunum tissue on the 3rd day post-change. Result revealed that the phosphorylation of STING ($p < 0.05$) and IRF3 ($p < 0.01$) in LP group were

significantly elevated to compare with the control group. Furthermore, p-STING ($p < 0.05$) and p-IRF3 ($p < 0.01$) in LP + PoRV group also were shown a notable increase to compare with the PoRV group (Fig. 6a-c).

Discussion

The host innate immune system is rapidly mobilized through recognition of pathogen-associated molecular patterns (PAMPs) by pattern recognition receptors (PRRs). This recognition event triggers downstream signaling cascades to induce IFN-I production [21]. Type I interferons (IFN-I) constitute the host's first line of defense against viral infection [22]. They are induced mainly by Toll-like receptors (TLRs), Rig-I-like receptors (RLRs), and the cyclic GMP-AMP synthase (cGAS) in response to extracellular microbes, microbial RNA and DNA inside the cell, respectively [23]. Some lactic acid bacteria (LAB) are recognized by TLR2/3 in endosomal compartment to induce the production of IFN-I via activating NF- κ B [24–25]. However, different LAB species induce specific innate immunity, that triggering IFN-I response fail to activating NF- κ B. Emerging evidences indicate that cytosolic DNA from LAB via membrane vesicles-mediated delivery, are mainly sensed by cGAS to initiate STING-dependent signaling pathways, to a less extent, MAVS [20, 23]. As a key downstream mediator of STING, IRF3 is a well-defined signaling molecule and transcription factor essential for innate antiviral responses. After STING activation, IRF3

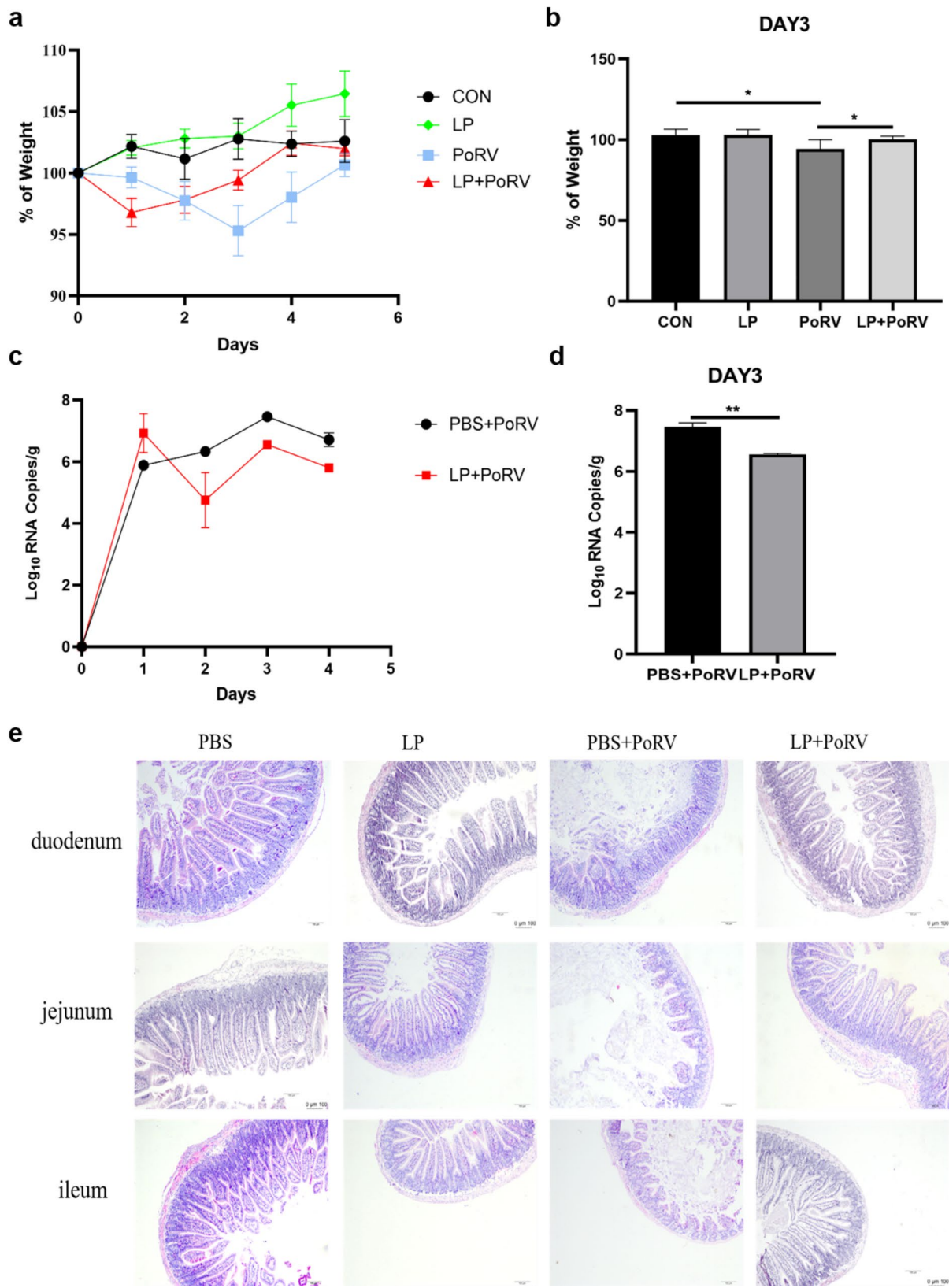


Fig. 3 Effects of LP1 treatment in mice challenged with PoRV. After 6 days of continuous intragastric administration of LP (2×10^8 CFU / mL, 0.1mL) or PBS, mice were infected with 2×10^6 TCID₅₀ PoRV ($n=6$ mice per group). **(a-b)** Body weight loss rate of mice after viral challenge. **(c-d)** Fecal samples were tested for viral shedding. **(e)** HE staining of different intestinal segments (including duodenum, jejunum and ileum) of mice ($\times 100$). Data are shown as mean \pm SD. * $p < 0.05$, ** $p < 0.01$, ^{ns} no significant

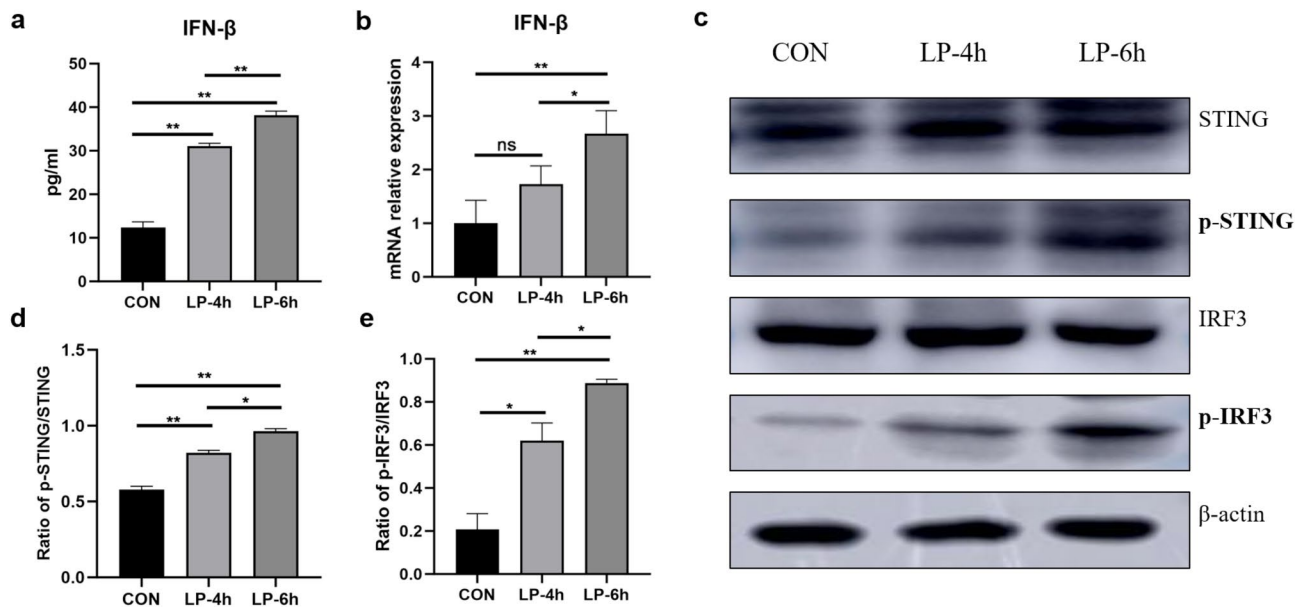


Fig. 4 LP1 activated the STING-IFN-I signaling pathway to trigger IFN- β production. IPEC-J2 were exposed to LP1 at a ratio (bacteria to cell) of 100:1 for 4 and 6 h, respectively. **(a)** Cell supernatant was collected to measure IFN- β production using ELISA. **(b)** The mRNA of IFN- β was determined by qPCR. **(c–e)** The expression and the phosphorylation of STING and IRF3 was detected by Western blotting. All the experiments were repeated three times with similar results. Data are shown as mean \pm SD; $n=3$. * $p < 0.05$, ** $p < 0.01$, ns no significant

is phosphorylated and translocated to the perinuclear region to induce IFN-I expression [26]. In this study, a swine-derived *Lactobacillus plantarum* strain (LP1) exerted the potent antiviral activity against PoRV in porcine intestinal epithelial cells and in a murine model. Notably, LP1 activated STING-IRF3 axis to induce robust IFN-I production. These results align with previous studies showing that some probiotics deliver DNA into host cell to activate cGAS-STING-IFN-I pathway. In addition to DNA, cyclic dinucleotides (CDNs) produced by bacteria may traverse the cell membrane to activate STING directly triggering IRF3-IFN-I [27]. Although LAB can synthesize CDNs in some literature, very little is known about their role in innate immune responses [28].

In our study, *Lactobacillus plantarum* LP1 significantly enhanced phosphorylation of both STING and IRF3 in IPEC-J2 cells, accompanied by marked upregulation of IFN- β at both the transcriptional and protein levels. These findings support the notion that LP1 exhibits its antiviral effects, at least in part, through the activation of the STING-IFN-I axis. Notably, STING has been shown to restrict RNA viruses such as vesicular stomatitis virus, Sendai virus, Newcastle disease virus, and influenza virus through IFN- β induction [29]. Certain viruses have evolved mechanisms to inhibit this pathway, for instance, the VP1 protein of chicken infectious anemia virus (CIAV) suppresses IFN-I production by blocking TBK1 activation in the cGAS-STING cascade [30]. Some study indicated that retroviral HIV can reverse transcribe RNA to DNA, which is subsequently recognized by the

cGAS-STING pathway [31]. Additionally, other research has demonstrated that RNA viruses can activate STING directly, independent of cGAS [32]. In our investigation, PoRV infection alone induced modest phosphorylation of STING and IRF3 and a corresponding increase in IFN- β levels. However, the combination of PoRV with LP1 treatment resulted in significantly stronger activation of these pathways, suggesting that LP1 amplifies antiviral signaling through STING.

Probiotics contribute to antiviral defense by enhancing innate immune responses, reducing viral load and persistence, and facilitating viral clearance. A probiotic mixture containing *Lactobacillus rhamnosus* CCFM1279, *Lactobacillus reuteri* CCFM1145, and *Lactobacillus casei* CCFM1127 has been shown to inhibit H1N1 influenza virus replication and attenuate associated lung inflammation in murine models [33]. In addition, certain *Lactobacillus* strains exert antiviral effects against respiratory syncytial virus (RSV) infection, largely through the upregulation of IFN- β expression in pulmonary tissues [34]. In our study, pretreatment with LP1 significantly decreased PoRV copy numbers and viral titers in IPEC-J2 cells, indicating that LP1 suppresses viral replication in vitro. In vivo, LP1 administration alleviated PoRV-induced intestinal villus atrophy and preserved intestinal wall thickness, suggesting a protective effect on mucosal structure and function. These histological improvements were accompanied by reduced viral shedding in feces, most notably on the third day post-infection.

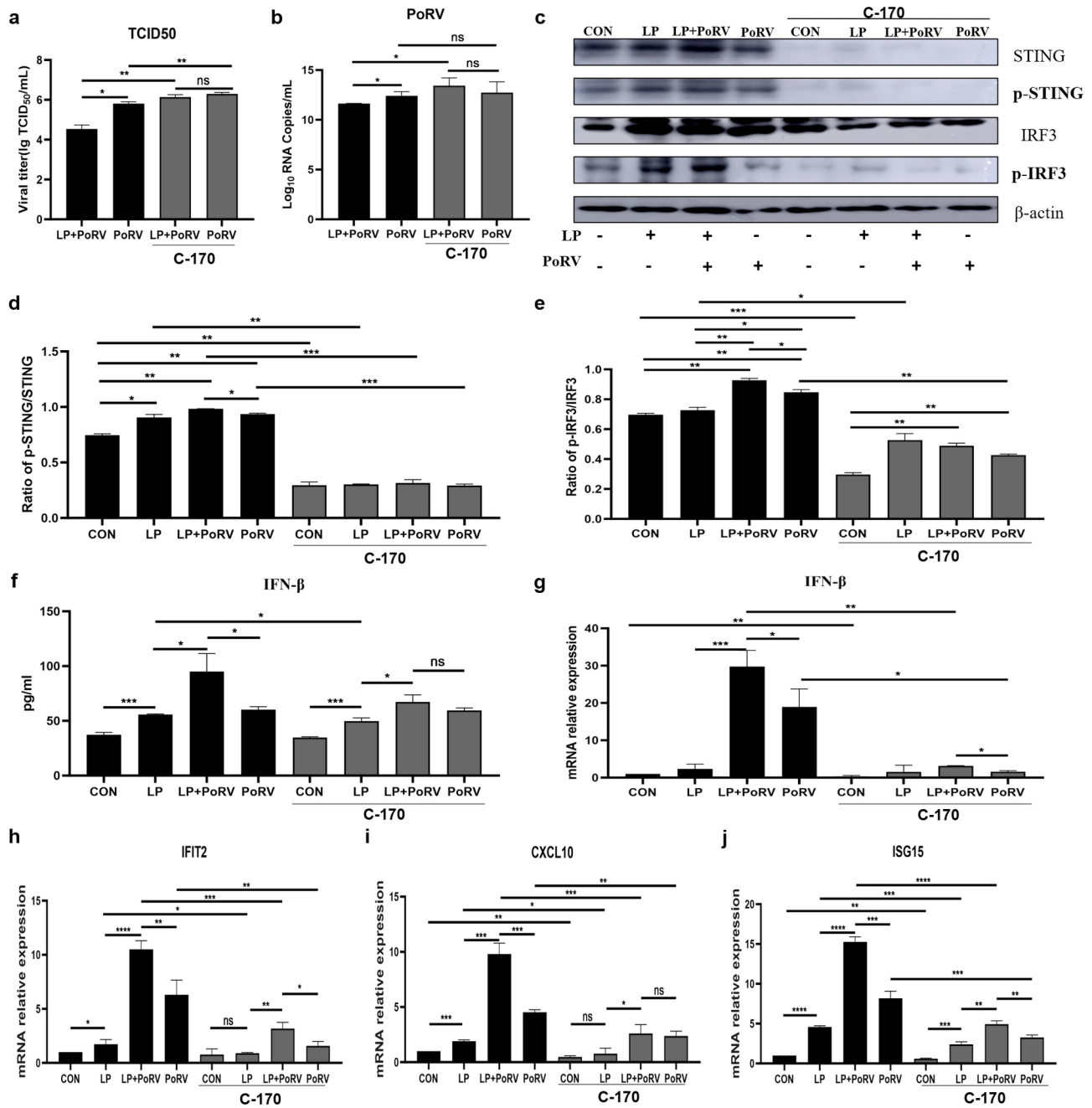


Fig. 5 LP1 enhanced antiviral effect mainly depended on STING. After incubating with or without STING inhibitor (C-170, 1 μ M) for 2 h, LP was cocultured with IPEC-J2 for another 6 h and subsequently infected with PoRV for 12 h. **(a)** The viral titer of PoRV in IPEC-J2 was assessed by TCID₅₀. **(b)** PoRV copy number was analyzed through detecting the non-structural protein 4 (NSP4) by qPCR. **(c–e)** The expression and phosphorylation of STING and IRF3 was analyzed by western blotting. **(f–g)** The secretion and mRNA of IFN- β was determined by ELISA and qPCR. **(h–j)** Total RNA was extracted and reverse transcribed for RT-qPCR to measure the transcription of ISGs including IFIT2, CXCL10, ISG15. Data are shown as mean \pm SD; $n=3$. * $p < 0.05$, ** $p < 0.01$, *** $p < 0.001$, ^{ns} no significant

Notably, antiviral mechanisms differ substantially among probiotic species. Live *Pediococcus pentosaceus* and *Lactobacillus plantarum* have been shown to induce robust type I interferon responses. In contrast, strains such as *Streptococcus thermophilus*, *Pediococcus acidilactici*, *Lactobacillus sakei*, and *Lactobacillus casei* fail

to activate IFN-I signaling, irrespective of their viability status [20]. These observations underscore the strain-specific nature of antiviral activity and highlight the need for mechanistic dissection.

Based on the antiviral effects induced by LP1, we further investigated whether this effect is dependent on

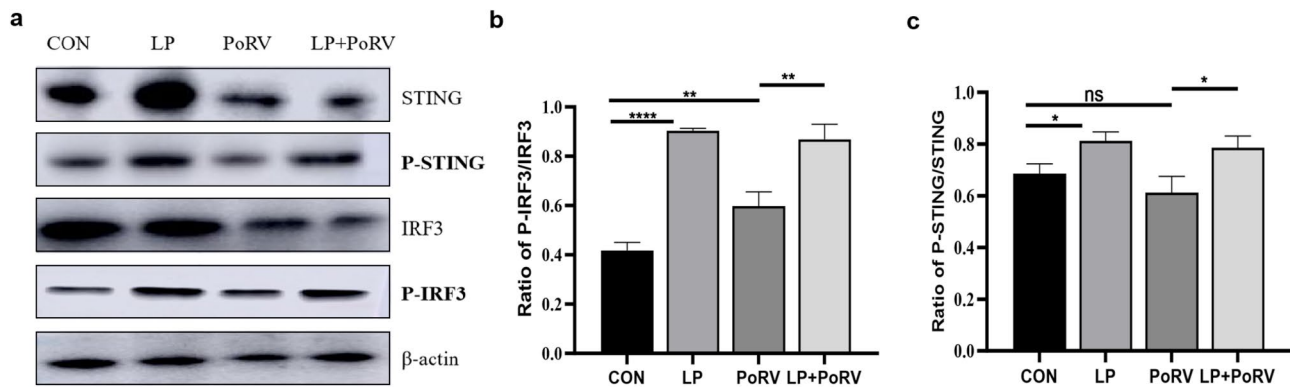


Fig. 6 The phosphorylation of STING (p-STING) and IRF3 (p-IRF3) proteins in mice following LP treatment. After 6 days of oral gavage administration of LP (2×10^8 CFU/mL, 0.1 mL) or PBS, the mice were subsequently infected with 2×10^6 TCID₅₀ PoRV ($n=6$ mice per group). (a–c) The phosphorylation STING and IRF3 proteins in the lysate of mouse jejunum tissue, as determined by western blotting. Data are shown as mean \pm SD. * $p < 0.05$, ** $p < 0.01$, *** $p < 0.001$, ^{ns} indicated no significant

STING by employing a pharmacological inhibition strategy. Treatment with the STING inhibitor C-170 significantly reduced both the transcription and secretion of IFN- β . Under these conditions, LP1 lost its capacity to inhibit PoRV replication, indicating that STING is a key mediator of LP1-driven antiviral responses. However, the suppression of STING did not completely abolish IFN- β expression, suggesting that additional pathways may be involved. Pathogen-derived nucleic acids can activate cytosolic pattern recognition receptors (PRRs), including RIG-I and MDA5, which signal through MAVS to induce the production of type I interferons [35]. Relevant study demonstrates that *Lactobacillus rhamnosus* GG restricts HSV-2 infection by promoting IFN-I responses via the RIG-I pathway [36]. There is also evidence of crosstalk between STING and MAVS signaling, with STING deficiency attenuating RIG-I/MAVS-mediated induction of IFN- β [37]. Based on these findings, we propose that LP1 may partially activate alternative signaling axes, such as RIG-I/MDA5-MAVS-IRF3, to sustain IFN- β production. In summary, our data identify STING as a central regulator of LP1-mediated antiviral immunity, while also pointing to potential involvement of additional nucleic acid sensing pathways. Further investigation is warranted to fully elucidate the molecular networks.

Collectively, our findings establish LP1 as an effective probiotic agent capable of limiting PoRV infection through activation of the STING-IFN-I signaling pathway. By demonstrating a STING-dependent mechanism of IFN- β induction, this study provides mechanistic insight into the antiviral potential of *Lactobacillus plantarum*. These results not only advance our understanding of host-microbe interactions in antiviral defense but also lay the groundwork for the rational design of probiotic-based interventions targeting enteric viral infections.

Conclusion

Lactobacillus plantarum (LP1), isolated from the intestines of piglets, demonstrates significant tolerance to both acidic and bile salts. LP1 effectively inhibits PoRV infection by activating the STING-IFN-I signaling pathway in IPEC-J2 cells and in mice, thereby providing protection against viral infection. These findings contribute valuable insights into the antiviral capabilities of *Lactobacillus plantarum* and its role in modulating innate immune responses to viral infections.

Materials and methods

Isolation of *Lactobacillus* from the intestine of the healthy post-weaning piglet

Healthy 25-day-old piglets were anesthetized using an intravenous injection of 6 mg/kg pentobarbital sodium. The intestinal contents were subsequently weighed and homogenized with sterile PBS buffer after a ten-fold dilution. *Lactobacillus* selective (LBS) and Man Rogosa Sharpe (MRS) agar were then employed to isolate *Lactobacillus* strains, which were incubated at 37 °C for 48 h under anaerobic conditions. The isolates were identified based on colony morphology, gram staining, and 16 S rDNA sequencing.

Acid and bile salt tolerance

The isolated *Lactobacillus* was cultured in MRS broth at 37 °C for 48 h under aseptic conditions, followed by centrifugation at 12,000 rpm for 2 min at 4 °C. The resulting pellet was re-suspended in MRS broth adjusted to pH 2. To assess bile salt tolerance, media containing bile salts at concentrations ranging from 0 to 0.45% (w/v) were prepared. The cultures were incubated at 37 °C for 36 h. Viable cell counts were determined after acid or bile salt exposure using the traditional plate count method.

Complete genome sequencing and analysis

The genome of LP1 was sequenced using Illumina HiSeq Novaseq and PacBio Sequel platform. Two DNA libraries were constructed: a paired-end library with an insert size of approximately 500 bp using TruSeq Nano DNA Kit (Illumina, USA) and a mate-pair library with an insert size of approximately 20 kb using Nextera DNA Library Preparation Kit (Illumina, USA). After sequencing, quality control of the raw reads was performed, which involved trimming the reads using Trimmomatic (version 0.20) and removing the Nextera adapter and linker sequences (for the mate-pair libraries) and TruSeq adapters (for the paired libraries); removing reads containing more than 10% of unknown nucleotides (N); removing low quality reads containing more than 50% of low quality (Q-value ≤ 10) bases. The downstream data obtained by PacBio were pieced together using HGAP, and CANU software to obtain contig sequences. The high-quality data from the second generation were corrected for the third generation contig results using Pilon software and finally spliced to obtain the complete sequence. Functional annotation of the predicted genes was performed by similarity using BLAST against diverse public databases, including: the NCBI's non-redundant protein (Nr) database, UniProt/Swiss-Prot, Cluster of Orthologous Groups of proteins (COG), Kyoto Encyclopedia of Genes and Genomes (KEGG) and Protein Families (Pfam).

Cell culture

Monkey embryonic kidney cells (MA104) were cultured in DMEM supplemented with 1% Penicillin-Streptomycin (P/S) and 10% fetal bovine serum (FBS). The LP, MA104 cells, and porcine rotavirus (DN30209) were stored at the Jilin Provincial Engineering Research Center of Animal Probiotics. IPEC-J2 were maintained in DMEM/F12 medium containing 1% P/S and 10% FBS, kindly provided by Dongsheng Che (Key Laboratory of Animal Production and Product Quality and Safety, Jilin Agricultural University, China).

Cell viability assay

Cell viability was assessed using the cell counting kit-8 (CCK-8), following the protocol outlined in a previous study [38]. Briefly, IPEC-J2 cells were inoculated into a 96-well cell plate at a density of 5×10^4 cells per well, in triplicate, and incubated in a 5% CO₂ environment at 37 °C. LP1 at concentrations of 5×10^5 CFU or 5×10^6 CFU were subsequently co-cultured with IPEC-J2 cells for 1 h at ratios of 10:1 and 100:1 (LP-10 group and LP-100 group), respectively. Additionally, IPEC-J2 cells were co-cultured with LP for periods of 1, 4, and 6 h (LP-1 h group, LP-4 h group and LP-6 h group). After incubation, the cells were washed three times with PBS and cultured in 100 μ L of complete DMEM/F12 medium

supplemented with 10 μ L of CCK-8. The cells were then incubated for an additional hour at 37 °C, and the absorbance at 450 nm (OD₄₅₀) was measured using a Multiskan Go enzyme reader.

Apoptosis determination by flow cytometry

IPEC-J2 cells (2×10^6) were seeded into each well of a 6-well plate. Following cell attachment, the medium was replaced with fresh antibiotic-free medium. The cells were stimulated with LP at a concentration of 2×10^8 CFU for 4 h and 6 h, respectively. Subsequently, the cells were collected by centrifugation at 1000 rpm for 5 min and stained with PE and Annexin V according to the protocol provided by the Apoptosis Detection Kit (BD Biosciences). Data were collected using an LSR II flow cytometer (BD Biosciences) and analyzed with FlowJo software (FlowJo LLC).

ELISA

PoRV was utilized to infect IPEC-J2 cells, both with and without prior treatment with LP. After a 12-hour incubation period, the culture medium was collected and analyzed for IFN- β production using a swine IFN- β ELISA kit (MEIMIAN), following the manufacturer's instructions.

RNA extraction and qPCR assay

Total RNA was extracted from IPEC-J2 cells and intestinal tissue using TRIZOL reagent (TaKara). Following the manufacturer's protocols, the PrimeScript™ RT reagent kit with gDNA eraser (TaKara) was utilized for RNA reverse transcription. Subsequently, RT-qPCR analysis was conducted using the SYBR green PCR master mix kit (TaKara).

Virus titer

2×10^5 IPEC-J2 cells were seeded per well in a 96-well plate supplemented with 100 μ L of DMEM/F12 medium (containing 10% FBS) and cultured for 24 h. The virus solution was prepared as a ten-fold serial dilution, which was subsequently added to the 96-well plate, with 8 replicates for each dilution gradient. The cells were observed continuously for one week until cytopathic changes were noted. The Muench method was employed to calculate the TCID₅₀ value (Reed and Muench).

Western blot

Protein samples were extracted from cells or intestinal tissue using RIPA lysis buffer (Beyotime Biotechnology), and the protein concentration was measured with a BCA protein assay kit (Beyotime Biotechnology). A total of 20 μ g of protein samples were separated using a 10% SDS-PAGE gel and subsequently transferred to PVDF membranes (EMD Millipore). The membranes

were blocked with 5% bovine serum albumin (BSA) for 1 h at room temperature. After blocking, the 5% BSA was removed, and the membranes were incubated overnight at 4 °C with primary antibodies, including anti- β -actin (1:5,000; Abcam), anti-STING (1:2,000; Abcam), anti-phosphorylated STING (1:2,000; Abcam), anti-IRF3 (1:2,000; Abcam), and anti-phosphorylated IRF3 (1:2,000; Abcam). The following day, the membranes were incubated with a secondary antibody (1:2,000; Proteintech) at 20–22 °C for 1 h. The protein bands were visualized using a chemiluminescence substrate (Beyotime Biotechnology) and analyzed with ImageJ version 1.46.

Animal experiments

Three to four-week-old female C57BL/6 mice were obtained from Changchun Yisi Experimental Animal Technology Co., Ltd. The animals were provided with access to water and pelleted food. Briefly, the mice were randomly divided into four groups ($n = 6/\text{group}$), including CON, LP, PBS + PoRV, and LP + PoRV groups. (1) CON group: intragastric administration of 100 $\mu\text{L}/\text{day}$ PBS for 6 days. (2) LP group: intragastric administration of 100 $\mu\text{L}/\text{day}$ LP (2×10^8 CFU) for 6 days. (3) PoRV group: intragastric administration of PBS, as in the CON group, followed by intragastric challenge with 300 μL of PoRV (2×10^6 TCID₅₀) on day 7. (4) LP + PoRV group: intragastric administration of LP similar to LP group, followed by intragastric administration of PoRV. Mice weight was assessed daily, and fecal samples were collected for virus detection about 1 week post-viral challenge. The mice were euthanized following anesthesia via intraperitoneal injection of 1% pentobarbital sodium anesthetic (5 $\mu\text{L}/\text{g}$). These tissue samples were subsequently fixed in 4% formaldehyde, embedded in paraffin, and sectioned into 3- μm thick slices. The sections were stained with hematoxylin and eosin (H&E), and digital images were captured using light microscopy.

Statistical analysis

All data are presented as mean \pm standard deviation. Data of counts between the two groups were analyzed using an unpaired t-test. Statistical significance was processed using a one-way analysis of variance (ANOVA) with Tukey. All pictures were generated using the Graph-Pad Prism 8.0.1 software. * $p < 0.05$, ** $p < 0.01$, *** $p < 0.001$ were considered significant, and ns indicated no significance.

Supplementary Information

The online version contains supplementary material available at <https://doi.org/10.1186/s12917-025-04766-0>.

Supplementary Material 1

Supplementary Material 2

Supplementary Material 3

Supplementary Material 4

Supplementary Material 5

Supplementary Material 6

Supplementary Material 7

Supplementary Material 8

Supplementary Material 9

Supplementary Material 10

Supplementary Material 11

Supplementary Material 12

Supplementary Material 13

Supplementary Material 14

Supplementary Material 15

Author contributions

All authors contributed to the study conception and design. AS: conceptualization, methodology, software, writing. XS: conceptualization, methodology and editing. RL, ZT and JH: methodology and sample collection. SZ, LB, YS and ZL: reviewing and editing. JH and CW: reviewing and editing, project administration. All authors read and approved the final manuscript.

Funding

This study was funded by Jilin Province Science and Technology Project (20240601058RC and YDZJ202102CXJD029), China Agriculture Research System of MOF and MARA (CARS-35), and National Natural Science Foundation of China (U21A20261), China University Student Science and Technology Fund Innovation Project (202210193057).

Data availability

No datasets were generated or analysed during the current study.

Declarations

Ethics and consent to participate

The experiments and all procedures involving animals were approved by the Animal Welfare and Research Ethics Committee of the Jilin Agricultural University. All animals were housed in a specific pathogen-free (SPF) animal house of the Experimental Animal Center of Jilin Agricultural University (JLAU20210423001).

Consent for publication

All authors have approved of the consents of this manuscript.

Competing interests

The authors declare no competing interests.

Received: 15 January 2024 / Accepted: 17 April 2025

Published online: 03 May 2025

References

- Odenwald MA, Turner JR. Intestinal permeability defects: is it time to treat? Clin Gastroenterol H. 2013;11(9):1075–83.
- Matthijnssens J, Ciarlet M, Heiman E, Arijis I, Delbeke T, McDonald SM, Palombo EA, Iturriza-Gomara M, Maes P, Patton JT, et al. Full genome-based classification of rotaviruses reveals a common origin between human Wa-Like and Porcine rotavirus strains and human DS-1-like and bovine rotavirus strains. J Virol. 2008;82(7):3204–19.
- Ramig RF. Pathogenesis of intestinal and systemic rotavirus infection. J Virol. 2004;78(19):10213–20.

4. Glass RI, Parashar UD, Bresee JS, Turchio R, Fischer TK, Widdowson MA, Jiang B, Gentsch JR. Rotavirus vaccines: current prospects and future challenges. *Lancet*. 2006;368(9532):323–32.
5. Kattoor JJ, Saurabh S, Malik YS, Sircar S, Dhama K, Ghosh S, Banyai K, Kobayashi N, Singh RK. Unexpected detection of Porcine rotavirus C strains carrying human origin VP6 gene. *Vet Quart*. 2017;37(1):252–61.
6. Pen G, Yang N, Teng D, Mao R, Hao Y, Wang J. A review on the use of antimicrobial peptides to combat Porcine viruses. *Antibiotics-Basel*. 2020;9(11).
7. Trask SD, Ogden KM, Patton JT. Interactions among capsid proteins orchestrate rotavirus particle functions. *Curr Opin Virol*. 2012;2(4):373–9.
8. Perez-Lopez A, Behnsen J, Nuccio SP, Raffatellu M. Mucosal immunity to pathogenic intestinal bacteria. *Nat Rev Immunol*. 2016;16(3):135–48.
9. Odenwald MA, Turner JR. The intestinal epithelial barrier: a therapeutic target? *Nat Rev Gastro Hepat*. 2017;14(1):9–21.
10. Vlasova AN, Kandasamy S, Chattha KS, Rajashekara G, Saif LJ. Comparison of probiotic lactobacilli and bifidobacteria effects, immune responses and rotavirus vaccines and infection in different host species. *Vet Immunol Immunop*. 2016;172:72–84.
11. Dowarah R, Verma AK, Agarwal N. The use of *Lactobacillus* as an alternative of antibiotic growth promoters in pigs: A review. *Anim Nutr*. 2017;3(1):1–6.
12. Liao SF, Nyachoti M. Using probiotics to improve swine gut health and nutrient utilization. *Anim Nutr*. 2017;3(4):331–43.
13. Lopez-Santamarina A, Lamas A, Del CMA, Cardelle-Cobas A, Regal P, Rodriguez-Avila JA, Miranda JM, Franco CM, Cepeda A. Probiotic effects against virus infections: new weapons for an old war. *Foods*. 2021;10(1).
14. Yue Y, He Z, Zhou Y, Ross RP, Stanton C, Zhao J, Zhang H, Yang B, Chen W. *Lactobacillus plantarum* relieves diarrhea caused by enterotoxin-producing *Escherichia coli* through inflammation modulation and gut microbiota regulation. *Food Funct*. 2020;11(12):10362–74.
15. Li K, Yang M, Tian M, Jia L, Du J, Wu Y, Li L, Yuan L, Ma Y. *Lactobacillus plantarum* 17–5 attenuates *Escherichia coli*-induced inflammatory responses via inhibiting the activation of the NF-kappaB and MAPK signalling pathways in bovine mammary epithelial cells. *BMC Vet Res*. 2022;18(1):250.
16. Chai W, Burwinkel M, Wang Z, Palissa C, Esch B, Twardziok S, Rieger J, Wrede P, Schmidt MF. Antiviral effects of a probiotic *Enterococcus faecium* strain against transmissible gastroenteritis coronavirus. *Arch Virol*. 2013;158(4):799–807.
17. Sirichokchatchawan W, Temeeyasen G, Nilubol D, Prapasarakul N. Protective effects of Cell-Free supernatant and live lactic acid Bacteria isolated from Thai pigs against a pandemic strain of Porcine epidemic diarrhea virus. *Probiotics Antimicro*. 2018;10(2):383–90.
18. Kim K, Lee G, Thanh HD, Kim JH, Konkrit M, Yoon S, Park M, Yang S, Park E, Kim W. *J Dairy Sci*. 2018;101(7):5702–12.
19. Wang J, Lin Z, Liu Q, et al. Bat employs a conserved MDA5 gene to trigger antiviral innate immune responses. *Front Immunol*. 2022;13:904481.
20. Gutierrez-Merino J, Isla B, Combes T, et al. Beneficial bacteria activate type-I interferon production via the intracellular cytosolic sensors STING and MAVS. *Gut Microbes*. 2020;11(4):771–88.
21. An SS-GJ, Elkon KB. Role of the cGAS–STING pathway in systemic and organ-specific diseases. *Nat Rev Nephrol*. 2022;18(9):558–72.
22. Lei Miao J, Qi Q, Zhao, et al. Targeting the STING pathway in tumor-associated macrophages regulates innate immune sensing of gastric cancer cells. *Theranostics*. 2020;10(2):498–515.
23. Saskia F, Erttmann P, Swacha KM, Aung, et al. The gut microbiota prime systemic antiviral immunity via the cGAS-STING-IFN-I axis. *Immunity*. 2022;55(5):847–e86110.
24. Gudrun Weiss K, Maetoft-Udsen SA, Stifter, et al. MyD88 drives the IFN-β response to *Lactobacillus acidophilus* in dendritic cells through a mechanism involving IRF1, IRF3, and IRF7. *J Immunol*. 2012;189(6):2860–8.
25. Tadaomi Kawashima A, Kosaka Y. Double-Stranded RNA of intestinal commensal but not pathogenic Bacteria triggers production of protective Interferon-β. *Immunity*. 2013;38(6):1187–97.
26. Jianzhong Shi J, Guan M, Chen, et al. Targeting IRF3 as a YAP agonist therapy against gastric cancer. *J Exp Med*. 2018;215(2):699–718.
27. Rutger D, Luteijn, Shivam A, Zaver BG, Gowen, et al. SLC19A1 transports immunoreactive Cyclic dinucleotides. *Nature*. 2019;573(7774):434–8.
28. Konstantinos Papadimitriou Ángel, Alegría PA, Bron, et al. Stress physiology of lactic acid Bacteria. *Microbiol Mol Biol Rev*. 2016;80(3):837–90.
29. Miyu Moriyama T, Koshiba T, Ichinohe. Influenza A virus M2 protein triggers mitochondrial DNA-mediated antiviral immune responses. *Nat Commun*. 2019;10(1):0–0.
30. Chen J-C, Xu Y, Ma Z, et al. Chicken infectious anemia virus (CIAV) VP1 antagonizes type I interferon (IFN-I) production by inhibiting TBK1 phosphorylation. *Virus Res*. 2023;327(0):199077–199077.
31. Tatsushi Ishizuka P, Kanmani H, Kobayashi, et al. Immunobiotic bifidobacteria strains modulate rotavirus immune response in Porcine intestinal epitheliocytes via pattern recognition receptor signaling. *PLoS ONE*. 2016;11(3):e0152416–0152416.
32. Rebecca P, Sumner L, Harrison E, Touizer, et al. Disrupting HIV-1 capsid formation causes cGAS sensing of viral DNA. *EMBO J*. 2020;39(20):0–0.
33. Hongchao Wang Y, Zhao Z, Pei, et al. Effect of mixed probiotics on alleviating H1N1 influenza infection and regulating gut microbiota. *Foods*. 2024;13(19):3079–3079.
34. Qianwen Wang Z, Fang L, Li, et al. *Lactobacillus mucosae* exerted different antiviral effects on respiratory syncytial virus infection in mice. *Front Microbiol*. 2022;13(0):0–0.
35. Lilliana, Radoshevich. Olivier dussurget. Cytosolic innate immune sensing and signaling upon infection. *Front Microbiol*. 2016;7(0):0–0.
36. Wang J, Huang M, Du Y, et al. *Lactobacillus rhamnosus* GG regulates host IFN-I through the RIG-I signalling pathway to inhibit herpes simplex virus type 2 infection. *Probiotics Antimicrob Proteins*. 2023;0(0):0–0.
37. Xiaotong Chang X, Shi X, Zhang, et al. IFI16 inhibits Porcine reproductive and respiratory syndrome virus 2 replication in a MAVS-Dependent manner in MARC-145 cells. *Viruses*. 2019;11(12):1160–1160.
38. Danielle Leblanc Y, Raymond M-J, Lemay, et al. Effect of probiotic bacteria on Porcine rotavirus OSU infection of Porcine intestinal epithelial IPEC-J2 cells. *Arch Virol*. 2022;167(10):1999–2010.

Publisher's note

Springer Nature remains neutral with regard to jurisdictional claims in published maps and institutional affiliations.